

USE OF LASER SCANNING CONFOCAL MICROSCOPY FOR QUANTITATIVE CHARACTERIZATION OF PHYSICAL CHANGES OF POLYMER COATINGS AFTER UV EXPOSURE

by

**Li-Piin Sung, Joan Jasmin, Xiaohong Gu, Tinh Nguyen,
and
Jonathan W. Martin**

**National Institute of Standards and Technology
Gaithersburg, MD 20899 USA**

**Reprinted from the Proceedings of the 81th Annual Meeting Technical Program of the FSCT,
Nov. 12-14, 2003, Pennsylvania Convention Center, Philadelphia, PA. Publisher: Federation of
Societies for Coatings Technology, 492 Norristown Rd., Blue Bell, PA 19422 USA.**

**NOTE: This paper is a contribution of the National Institute of Standards and Technology
and is not subject to copyright.**



NIST

National Institute of Standards and Technology
Technology Administration, U.S. Department of Commerce

USE OF LASER SCANNING CONFOCAL MICROSCOPY FOR QUANTITATIVE CHARACTERIZATION OF PHYSICAL CHANGES OF POLYMER COATINGS AFTER UV EXPOSURE

Li-Piin Sung, Joan Jasmin, Xiaohong Gu, Tinh Nguyen, and Jonathan W. Martin

*Polymeric Materials Group
Building and Fire Research Laboratory
National Institute of Standards and Technology
Gaithersburg, MD 20899-8615*

Abstract

Laser scanning confocal microscopy (LSCM) has become a powerful tool for monitoring physical changes in polymeric coatings following ultraviolet (UV) radiation exposure. Physical changes caused by UV exposure include film ablation, formation of pits and other surface defects, and increases in surface roughness. Physical changes as a function of exposure time were compared to chemical degradation measured with Fourier Transform Infrared (FTIR) spectroscopy. It was found that after 400 h of UV exposure, film thickness changes measured by LSCM were not correlated to the thickness predicted by chemical degradation in an acrylic urethane coating. Local physical changes (pit formation and surface deformation) were observed that might contribute to chemical changes.

Introduction

Understanding the mechanism and progress of UV degradation is one of the keys for predicting the service life of polymeric coatings. To achieve this objective, extensive research efforts¹⁻⁶ both in outdoor and indoor accelerated weathering exposures have been carried out to investigate the influences of various climatic parameters on coating degradation, and to further establish the correlation between physical and chemical degradation. Typically, appearance-related measurements, such as gloss retention and color fading, are used to assess physical degradation and define the failure of the weathered coatings. Spectroscopic measurements, such as Fourier Transform Infrared (FTIR) spectroscopy, are often used for monitoring chemical degradation occurring in an exposed coating. Most studies³⁻⁶ have focused on identifying primary chemical changes and assessing the rates of degradation under specific exposure conditions. The results have provided some understanding of the initial chemical degradation mechanism in the coatings.

However, the link between specific chemical and physical changes (for example: gloss loss) in a coating has remained elusive, and inconsistent results as shown by investigators have been reported for various coatings and exposure conditions (both in outdoor and accelerated weathering tests).^{2,7} Consequently, the lack of correlation between gloss loss and chemical changes measured by spectroscopy has severely limited the ability to

measure and predict service life accurately. Obviously, the difficulty in comparing FTIR results with gloss measurements is that no direct link has been established between the two measurements. The FTIR measures the concentration of chemical species in coating structures while the gloss measurement “sees” the surface morphology of a coating. To make reliable comparisons between the FTIR results and gloss measurements, the correlation between surface morphology and chemical changes must be investigated concurrently. Many attempts⁸⁻¹⁰ have been made to link surface morphology with gloss measurements and/or chemical changes. For example, using atomic force microscopy (AFM) VanLandingham et al.⁹ have attempted to relate the formation of pits and surface roughening of acrylic melamine coatings to hydrolysis in the early stages of exposures. In this case, no observable change in film thickness was detected. However, for later stages of degradation, the change in film thickness is also an important physical parameter for comparing against the chemical changes measured by FTIR.

AFM is a useful tool for characterizing nanoscale surface deformation in the early stages of physical degradation. However, with the maximum scanning area being limited to 100 μm x 100 μm , and the maximum measurable peak-to-valley height being less than 6 μm , AFM is not suitable for measuring the film thickness and surface morphology changes in the entire range of degradation. Destructive methods such as scanning electron microscopy (SEM) are often used to measure the final surface degradation and thickness of a film but it is not a practical method for monitoring changes in the same sample after different exposure times. Thus, a non-destructive, no-invasive tool such as interference microscopy or confocal microscopy is more suitable to monitor physical changes throughout the entire degradation process. Additionally, recent efforts at NIST¹¹⁻¹³ in linking the surface morphology and subsurface microstructure to optical reflectance properties of a coated material using ray scattering model have provided an approach to calculate and understand the optical reflectance (related to gloss values) for a given surface morphology/microstructure. By correlating the time evolution of the physical changes, such as thickness and surface deformation (pits and cracks), to the chemical changes of a UV exposed coating, we can quantify the process and understand the mechanism of degradation. With the methodology developed for modeling the optical reflectance from a given surface morphology or microstructure, we might be able to establish a “direct” correlation between failure assessment evaluated by gloss loss and chemical changes measured by spectroscopy.

In this research, the physical and chemical degradation of two UV-exposed coating systems - acrylic-urethane (AU) and acrylic-melamine (AM)- were studied. Physical changes caused by UV exposure, including film ablation, formation of pits, and other surface defects, were characterized by laser scanning confocal microscope (LSCM). The film thickness measured using LSCM was compared to the predicted film thickness obtained from changes in the CH band absorbance by FTIR measurement assuming uniform film ablation for both systems. Time evolution of surface morphology of UV-exposed coatings will be presented and related to FTIR chemical changes.

Experimental*

Materials and sample preparation

Two thermoset coating systems, acrylic-urethane (AU) and acrylic-melamine (AM), were used in this study. The acrylic-urethane coating consists of a mixture of hydroxy-terminated acrylic resin (PPG lot # 00123-19, a mixture of 70.2 % acrylic polymer and 29.8 % 2-heptanone) and an aliphatic isocyanate cross-linking agent (Desmondur N3200). The solid content ratio of acrylic resin to isocyanate cross-linking agent was 65:35. All percentages and proportions are expressed as mass fraction. To achieve a uniform film thickness of 10 μm or less by spin coating, the mixture was diluted in toluene to a final concentration of 60 % acrylic-urethane. After degassing, the solution was spin-casted onto a 101.6 mm diameter silicon substrate (double side polished silicon wafer) at 2000 rpm for 120 s. The coating films were then cured at 130° C for 2 hours. After the films were cured, the 101.6 mm dia. sample was cut into 12 specimens of 17 mm square size, which was suitable for UV exposure. Nine replicates were chosen and exposed under UV light. The physical and chemical changes due to UV degradation were monitored and characterized every week using AFM on three replicates, and using both LSCM and FTIR on the other 6 replicates. Three un-exposed samples were used for the thickness measurements using SEM and Interference microscopy techniques.

The acrylic-melamine (AM) coating films were prepared, cured, and conditioned using the same procedure. The acrylic-melamine coating consisted of a hydroxy-terminated acrylic resin (PPG lot# 00123-19) and a partially methylated melamine resin (Cytex industries Cymel 325). The solid content ratio of acrylic resin to melamine resin was 70:30.

UV exposure experiments

The UV exposure experiments were conducted using an Oriel Instruments solar simulator. The instrumentation of the UV exposure system has been described elsewhere.⁴⁻⁵ The UV exposure conditions used in this study was full UV light (approximately 1.3 sun) and 75 % \pm 3 % relative humidity (RH) at 50 °C \pm 0.5 °C. The light source is equipped with a 1000 W xenon arc lamp, and the wavelength ranges from approximately 270 nm to approximately 800 nm.

Fourier Transform Infrared Spectroscopy (FTIR)

Coating degradation was followed by FTIR spectroscopy in the transmission mode using an autosampling accessory. At each specified time, coated silicon plates were removed from the exposure cell and fitted into a demountable 150 mm diameter ring of the

* Certain instruments or materials are identified in this paper in order to adequately specify experimental details. In no case does it imply endorsement by NIST or imply that it is necessarily the best product for the experimental procedure.

autosampling device. The ring was computer-controlled and could be rotated and translated to cover the entire sampling area. Spring-loaded Delrin clips ensured that the specimens were precisely located and correctly registered. Detailed design of this autosampling system has been described elsewhere.⁵ Since the exposure cell was mounted precisely in the autosampler, error due to variation of sampling at different exposure times was essentially eliminated. The spectrometer compartment equipped with a liquid nitrogen-cooled mercury cadmium telluride (MCT) detector. Spectra were recorded at a resolution of 4 cm^{-1} using dry air as the purge gas. All spectra were the average of 132 scans.

Atomic Force Microscopy (AFM)

A Dimension 3100 Scanning Probe Microscope from Digital Instruments was operated in tapping mode to characterize the surface morphology of coating films before and after UV exposure. Commercial silicon microcantilever probes were used. Topographic and phase images were obtained simultaneously using a resonance frequency of approximately 300 kHz for the probe oscillation and a free-oscillation amplitude of $62\text{ nm} \pm 2\text{ nm}$. The set-point ratio (the ratio of set point amplitude to the free amplitude) ranged from 0.60 to 0.80.

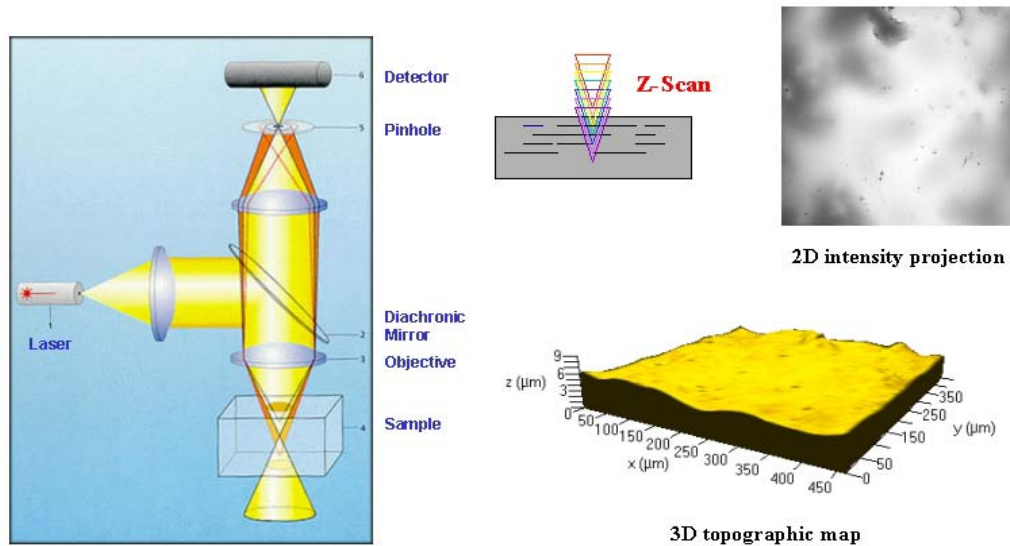


Figure 1. Schematics of a LSCM optical system and typical results in 2D intensity projection and 3D topography presentations.

Laser scanning Confocal Microscopy (LSCM)

A Zeiss model LSM510 reflection laser scanning confocal microscope (LSCM) was employed to measure the film thickness and characterize the surface morphology (topographic profile) of the coatings at various UV exposure times. As illustrated in Figure 1, LSCM utilizes coherent light and collects light exclusively from a single plane (a pinhole sits conjugated to the focal plane) and rejects light out of the focal plane. The wavelength, numerical aperture (N.A.) of the objective, and the size of the pinhole dictate

the resolution in the thickness or axial direction.¹³ By moving the focal plane, single images (optical slices) can be combined to build up a three dimensional stack of images that can be digitally processed. In this paper, LSCM images in 2D intensity projection or 3D topographic profile are representative of a series of overlapping optical slices (a stack of z-scan images) with each z-step of 0.1 μm . Without specification, each frame consists either of 512 pixels by 512 pixels or 184 μm by 184 μm by size. The laser wavelength used was 543 nm.

In addition to a typical frame-scanning mode to generate a topographic profile of the coatings, LSCM was used in the line-scanning mode to measure a cross-section profile through a clear coating as shown in Figure 2. As the first principle of ray reflection, ray 1 was reflected from the air-polymer interface, and ray 2 was reflected from the polymer-silicon interface, as illustrated in Figure 2. For normal incident condition and assuming no light absorption in the coatings, the reflected intensity of ray 1 and ray 2 can be expressed as follows:

$$I_{Ray1} = I_o \left(\frac{n_p - n_o}{n_p + n_o} \right)^2 ; I_{Ray2} = I_o \left(\frac{4n_p \times n_o}{(n_p + n_o)^2} \right)^2 \left(\frac{n_p - n_{si}}{n_p + n_{si}} \right)^2$$

Here I_o is the incident intensity, and n_o , n_p , n_{si} are the indices of reflection for air, polymer coatings, and silicon substrate. Strictly, one can deduce the value of n_p by calculating the relative intensity of I_{Ray1}/I_{Ray2} using the values of $n_o = 1$ and $n_{si} = 4.05$ at laser wavelength 543 nm. Then the coating thickness d_p equal to $n_p \times d_o$, where d_o is the distance between two interfaces measured by LSCM assuming traveling through a medium of reflection index of 1. Thickness measurements using SEM and Interference microscopy were also conducted, and the results from thees three techniques (LSCM, SEM, Interference microscopy) were consistent to within $\pm 0.5 \mu\text{m}$.

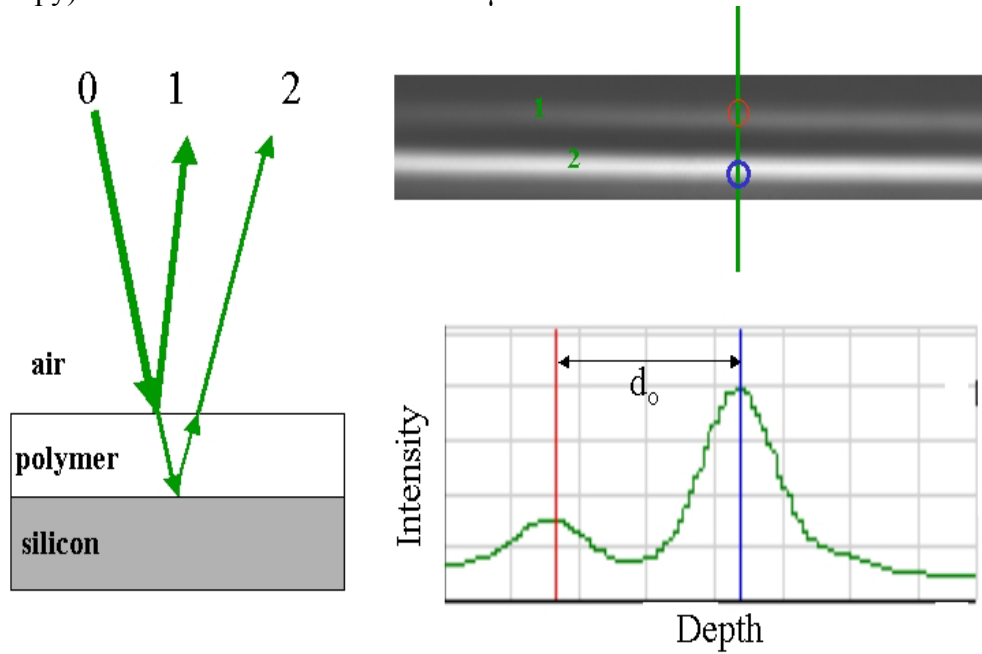


Figure 2. The illustration of the principle used for determining film thickness using LSCM line scans.

Results and Discussion

Chemical changes in UV exposed Acrylic-Urethane (AU) coatings

FTIR spectra of AU coatings before and after UV exposure to different times are shown in Figure 3. The low intensity interference fringes in the spectra are often used to determine the film thickness using the interval between the fringes.⁶ However, as film thickness decreased and the surface became rougher, the peak intensity and phase of interference fringes changed as well as the width of the peak (as shown in Figure 3). It then became problematic to determine the film thickness using the interference fringes. Thus, laser scanning confocal microscopy was used to determine the film thickness at any given exposure time, and the results are presented later.

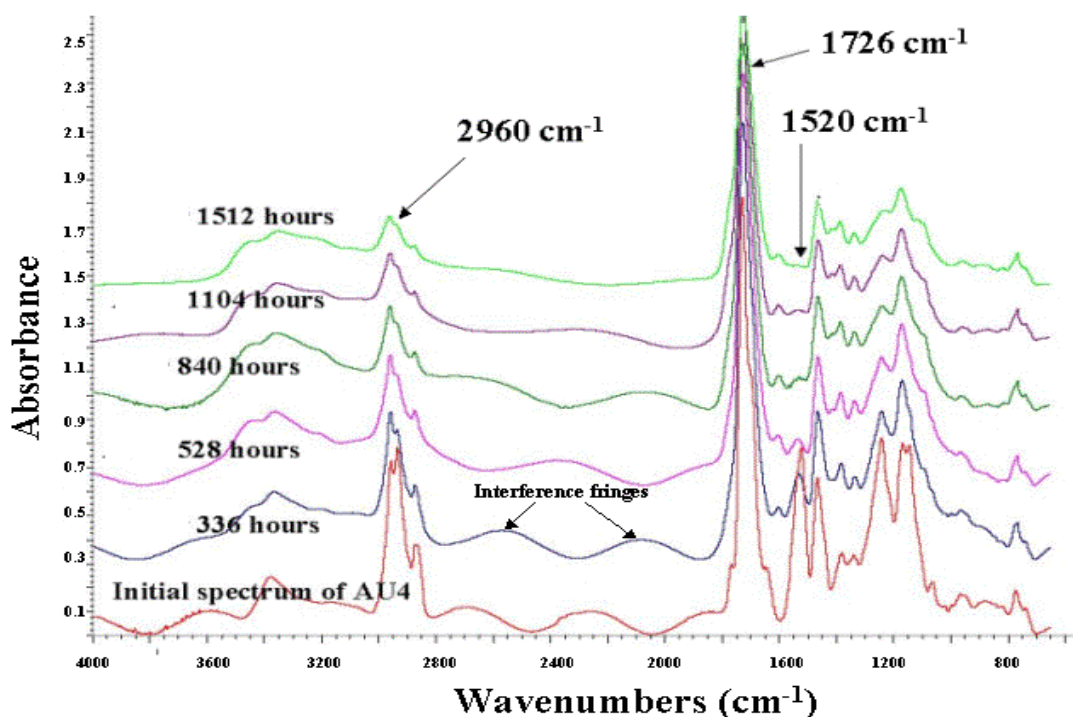


Figure 3. FTIR spectra of an Acrylic-Urethane (AU) coating at various UV exposure times.

Here we focus only on the time-evolution of three selected FTIR peaks related to the CH stretching band at 2960 cm^{-1} (mass loss), NH bending and CN stretching at 1520 cm^{-1} (chain scission), and the C=O band at 1726 cm^{-1} in the AU coatings. Clearly, the peak intensity (FTIR absorbance at peak maximum) of these bands decreased as exposure time increased (as shown in Figure 4). The relative loss of each peak, with respect to the initial absorbance at zero exposure time, is also plotted in the bottom graph. The 2960 cm^{-1} CH band lost about 4 % in intensity per hour; and the chain scission peak at 1520 cm^{-1} decreased rapidly with only 20 % left by 600 h, reaching a constant level (80 % loss)

afterward. Chemical changes are often presented as the relative rate of appearance or disappearance of a given FTIR band by normalizing to the CH band, on the assumption that the CH band is a measure of the amount of materials that remains. The mass change is assumed to be directly related to film thickness changes (the linear reduction in the coating thickness i.e. film ablation) as several researchers have indicated in their reports.^{3,6} Accordingly, this assumption implies that degradation is an ablation process taking place in a steady manner from an outer layer that remains consistent through the exposure period.

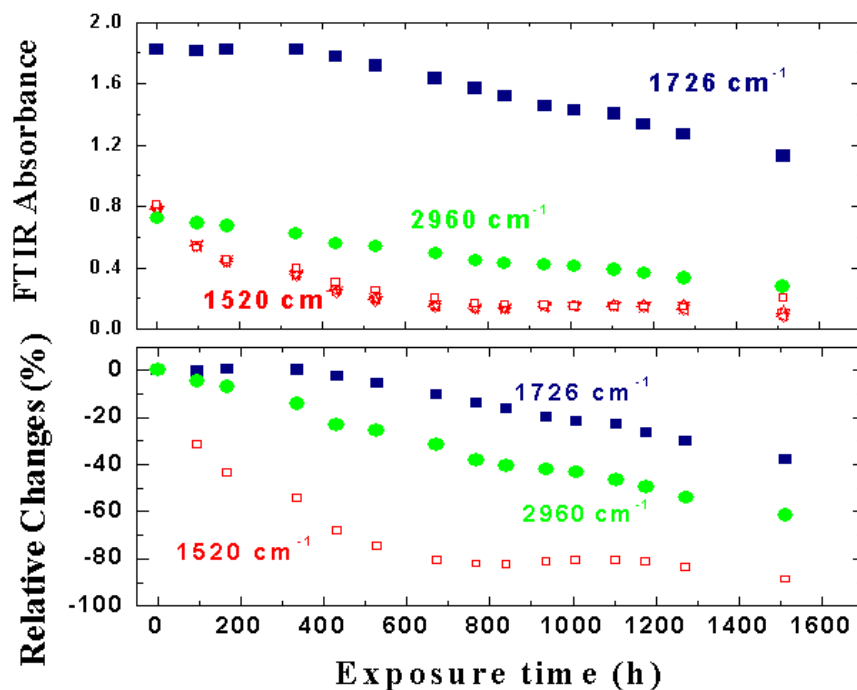


Figure 4. Upper graph shows three selected FTIR absorbance peak of AU coatings as function of UV exposure time; the bottom graph presents the relative changes for each peak. Uncertainty of data is estimated to be 2 % ($k=2$), the size of the error bar is smaller than the symbols.

Figure 5 compares the relative changes for the chain scission peak at 1520 cm^{-1} and loss of the C=O band at 1726 cm^{-1} with (solid symbols) and without (open symbols) normalized to the changes in the CH band. It is clear that without taking into account the mass loss (changes in CH band) in the process of the UV degradation the rate of chain scission is faster than that normalized by the CH band. Furthermore, for FTIR peaks changing slower than corresponding peaks in the CH band, it appears a growth profile instead a decay profile after normalized by the CH band. The results are conflicted and depend on the chosen normalizing factor. Thus, it is difficult to compare these results and understand degradation of these chemical changes. The real issue is to select a reference IR band which has a well-known characteristic property or remains constant in the UV

degradation process. One approach as suggested by Croll et al.⁶ is to use the film thickness, assuming film ablation occurred, as a normalized factor for analyzing chemical changes. However, in this approach, the thickness of the coatings and the surface morphology should be examined carefully to relate the chemical changes obtained from FTIR measurements to thickness and surface morphology measurements to understand the degradation mechanism.

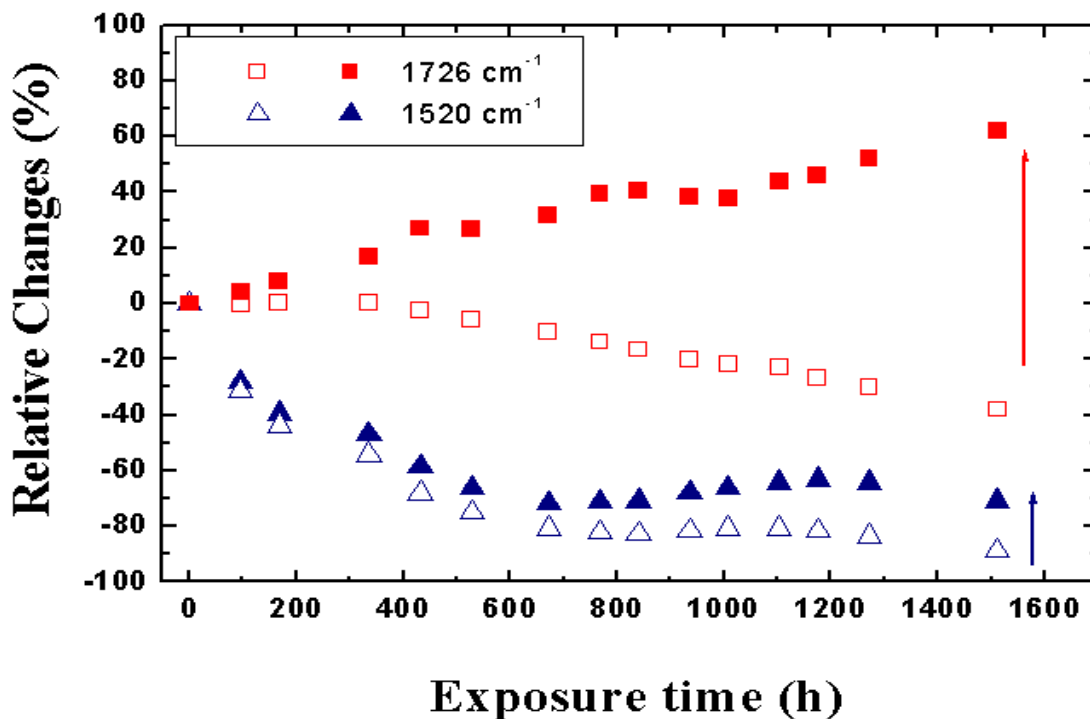


Figure 5. Relative changes the C=O band (1726 cm^{-1}) and chain scission (1520 cm^{-1}) with (solid symbols) and without (open symbols) normalized by the CH band at the same exposure time. The arrows indicate the direction of changes after taking into account of the changes in then CH band. Uncertainty of data is estimated to be 2 % ($k=2$), the size of the error bar is smaller than the symbols.

Thickness and surface morphology changes of UV exposed AU coatings

To compare with FTIR results, we have conducted the microscopy measurements at five different scanning locations on a sample with each scan location being at least 2 mm apart, as illustrated in the insert graph of Figure 6. At each scanning location (scan length $\sim 184\text{ }\mu\text{m}$), ten different thickness values were extracted. Thus, each data point in Figure 6 is the average value of as many as 50 different locations. The error bar represents the range of $k=2$ uncertainty (at 95 % confidence level). All samples followed the same trend. The film thickness decreased linearly (about 3 nm/h) in the early stages of degradation then slowly decreased to a constant value after 1100 h of UV exposure. The sample lost only 35 % of its original thickness after 1500 h of exposure compared to a 63

% loss as estimated using the CH band in FTIR measurement. This large discrepancy can be explained as follows: in the late stage (after 1100 h), the surface became rough, and the thickness values obtained were only from limited filled area that excluded pits and other surface deformation. However, the coatings maintained the same thickness but with increasing area of pits and holes on the surfaces.

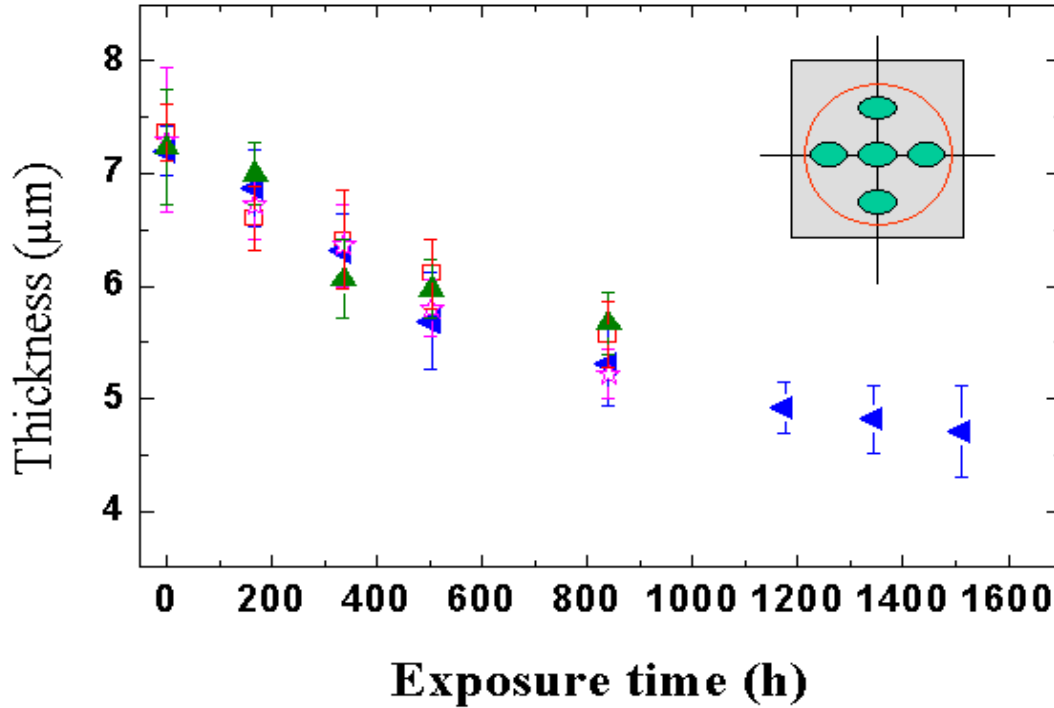


Figure 6. The film thickness obtained from 6 replicates of AU coatings measured using LSCM as a function of UV exposure time. The insert graph illustrates five different scanning locations on each sample.

Surface morphological changes were analyzed at various exposure times using LSCM and AFM. The changes in surface morphology and pit/hole formation are clearly demonstrated in Figures 7 and 8. Initially, the surface appeared to be smooth and featureless. As the exposure time increased, surface roughness increased and the appearance of pits/holes was observed. For example, the root-mean-square (rms) roughness value of the coating surface at 3,504 exposure hours was ten times larger than the rms surface roughness value at 864 exposure hours, as shown in Figure 8. The size of pits increased further and merged with other nearby pits. In the later stages, the film appeared to be very rough with pronounced surface patterns as a result of degradation. These local physical changes contribute mass changes and might be related to other

degradation processes. More analyses are underway to calculate surface roughness and relate to the results obtained from gloss measurements.

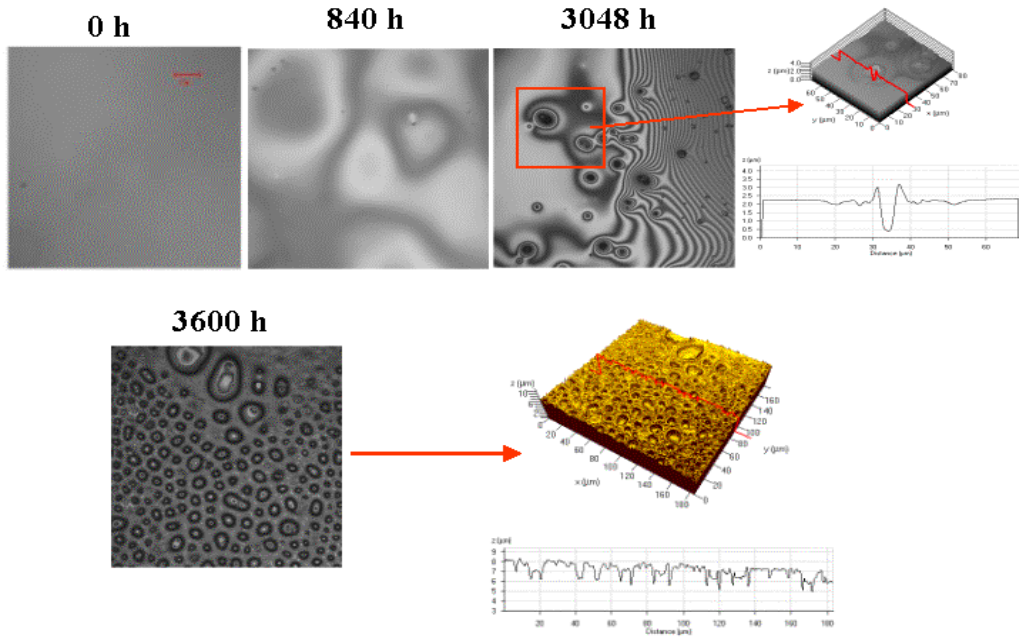


Figure 7. LSCM images (2D intensity projection) of Au film for 4 different exposure times. The corresponding topographic images and height information are also presented. Each LSCM micrograph consists of 512 pixels by 512 pixels and 184 μm by 184 μm by size.

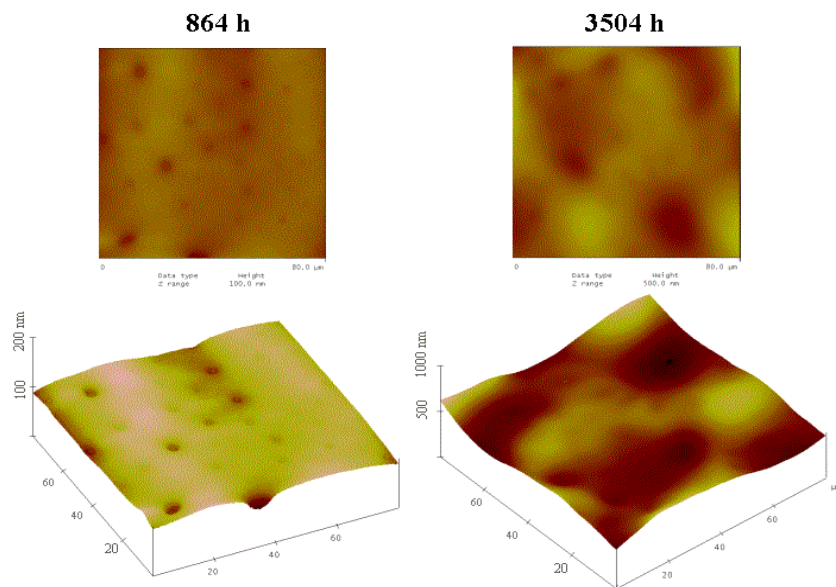


Figure 8. AFM images of the Au coatings at two different exposure times.

Correlation between Chemical and Physical changes of UV exposed AU coatings

With the observation of how the thickness and surface features changed in the UV degradation of the AU coating, the assumption does not seem to be correct that degradation and film ablation occurred in a steady manner from an outer layer that remains consistent through the exposure period. Thus, using a CH band as a normalizing factor for analyzing chemical changes in the UV degradation process might not be accurate. To evaluate the validity of using the film thickness as a normalizing parameter for analyzing FTIR spectra, we first compared the relative loss in the actual “measured” film thickness using LSCM to the “predicted” film thickness assuming mass loss (CH band at 2960 cm^{-1}) due to uniform film ablation.

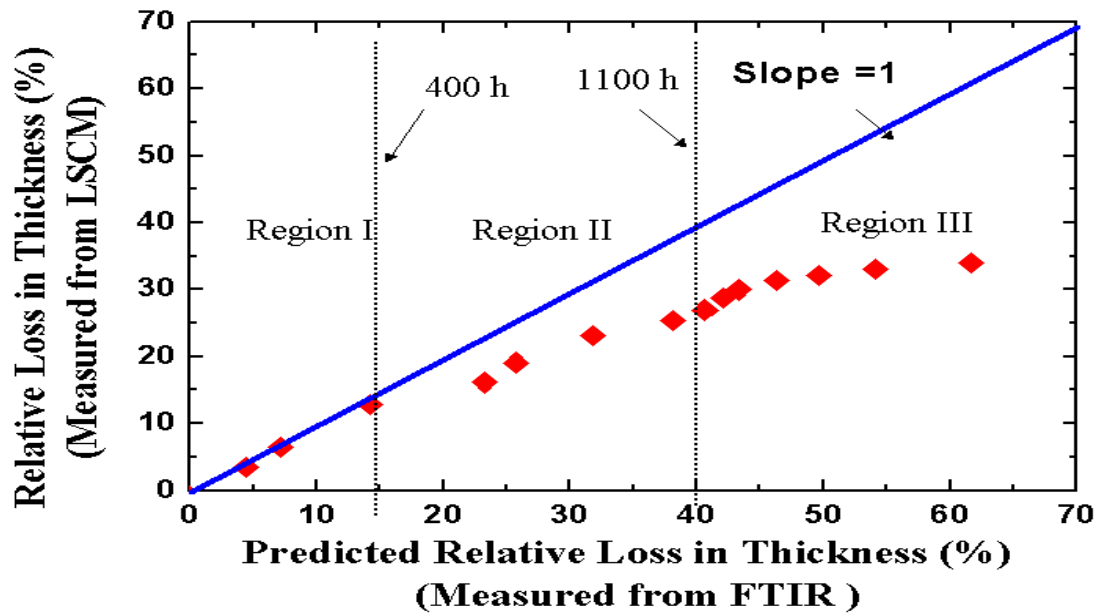


Figure 9. Comparison of the relative loss between the predicted values from FTIR peak at 2960 cm^{-1} and the measured values using LSCM. Uncertainty of data is estimated to be 7 % ($k=2$).

As shown in Figure 9, the relationship between relative loss in the “measured” and “predicted” film thickness followed the linear relationship (slope =1) for the initial state (region I), then deviated from the linear relationship after 400 h of exposure time. In conjunction with observation of surface morphology changes, we have cataloged the degradation process into three regions:

Region I ($t \leq 400\text{ h}$): the physical change was due to uniform film ablation; the mass loss was proportional to the loss in film thickness; no significant changes in surface morphology (pits were small and were not observed in the LSCM measurement). In this region, no changes in gloss would be expected.

Region II ($400 \leq t \leq 1100\text{ h}$): film thickness continued to decrease; pits started to form and grow (see AFM images), and the coating surface became rougher as exposure time

increased. Gloss loss should be expected in this region due to the surface roughening and pit formation.

Region III ($t \geq 1100$): the final stages of the physical degradation – pits merged with nearby pits/cracks, larger patterns formed, and surface roughness continued to increase. In this region, the thickness in the filled area remains the same. Continuous mass loss is due to the size of unfilled area (holes/cracks) increasing in the surface morphology.

These results imply that the correlation between film thickness changes and chemical changes follows a linear relationship only in region I (at early stages of the degradation process), but is not well established for the intermediate and late stages of the UV degradation process. In regions II and III, the actual film thickness was greater than the thickness predicted from FTIR results. Using the film thickness as a normalizing factor for analyzing degradation rates of all FTIR absorbance including the CH band have been used as an alternative method of quantifying the degradation process.⁶ Figure 10 shows the relative changes of the C=O band (1726 cm^{-1}), CH band (2960 cm^{-1}), and chain scission (1520 cm^{-1}) normalized by the LSCM measured film thickness at the same exposure time. Results presented in Figure 10 indicate that the C=O is essentially unchanged with exposure; this is not correct because substantial loss of this species has been observed (see Figures 3 and 4).

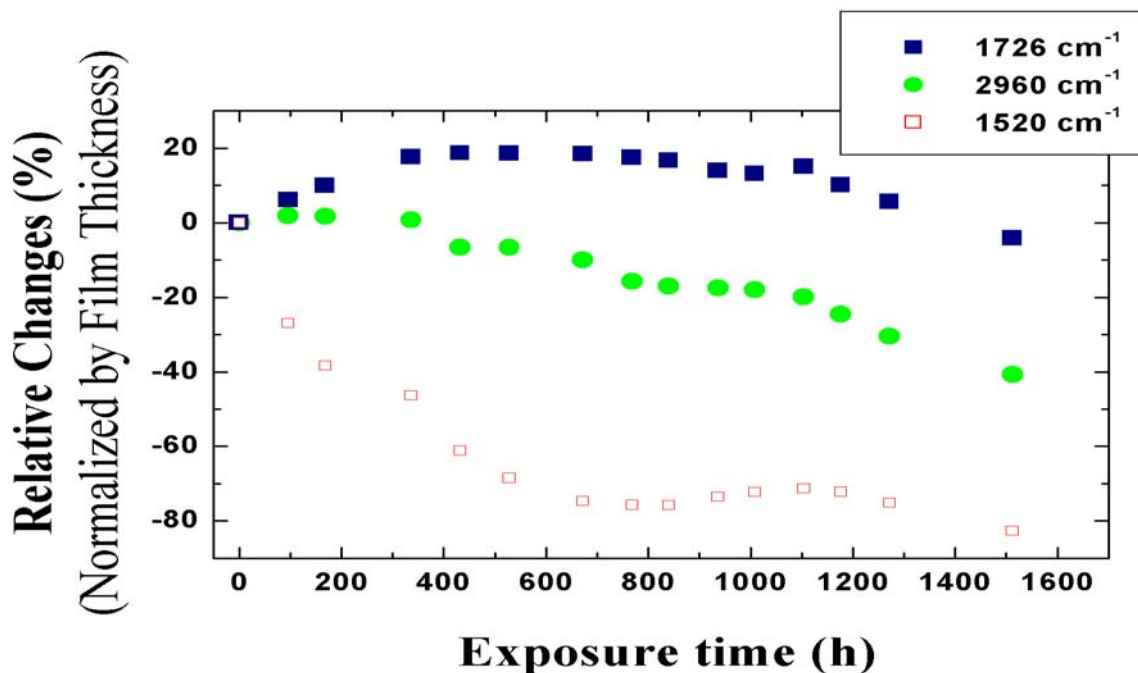


Figure 10. Relative changes in C=O band (1726 cm^{-1}), C-H band (2960 cm^{-1}), and chain scission (1520 cm^{-1}) normalized by the film thickness at the same exposure time. Uncertainty of data is estimated to be 2 % ($k=2$), the size of the error bar is smaller than the symbols.

Chemical and physical changes of UV exposed Acrylic-Melamine (AM) coatings

Six replicates of AM coatings were exposed under the same conditions used in the AU system. The upper graph of Figure 11 shows the chemical changes as a function of three selected FTIR absorbance peaks at 1555 cm^{-1} , 1730 cm^{-1} , and the 2960 cm^{-1} as a function of UV exposure time. The band at 1555 cm^{-1} is related to three different groups: triazine ring, CN attached to the ring, and CH_2 . The band at 1730 cm^{-1} corresponds to the C=O of the acrylic ester group, and the CH band of 2960 cm^{-1} reflects the mass of the coatings. It is clear that the 1555 cm^{-1} band degraded more rapidly than 2960 cm^{-1} and 1730 cm^{-1} bands, similar to the AU system. The bottom graph of Figure 11 shows the relative changes of both the 1555 cm^{-1} and 1730 cm^{-1} bands normalized by the absorbance of 2960 cm^{-1} at the same exposure time. As in the AU system, the proper parameter for FTIR normalization is not well established.

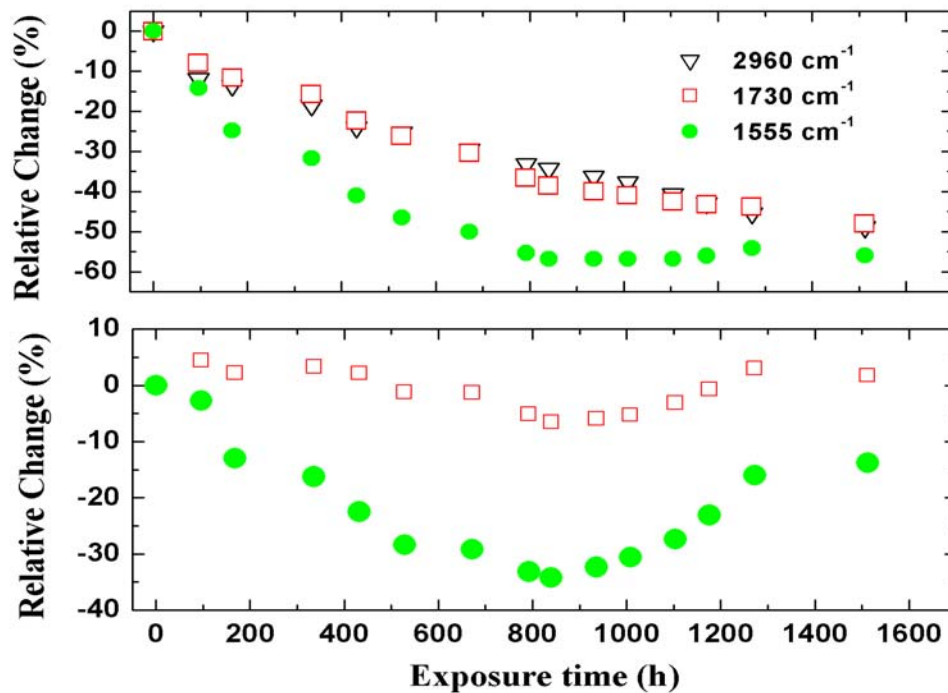


Figure 11. Upper graph: relative changes in FTIR absorbance peak at 2960 cm^{-1} , 1730 cm^{-1} , and 1555 cm^{-1} as function of UV exposure time for six AM coatings. Bottom graph: relative changes of 1730 cm^{-1} , and 1555 cm^{-1} band normalized by 2960 cm^{-1} band. Each data point is an average of six replicates, and the error bar is smaller than the symbols.

Figure 12 shows the LSCM film thickness measurements results (upper graph) for AM coatings and the correlation between the “measured” and “predicted” film thickness (bottom graph). In this system surface degradation occurred so dramatically, the film thickness in the measurable area remained almost the same (the error bars on the thickness measurement were large) after 200 h exposure time. Note that the degradation rate of the AM coating was much faster than that of the AU coating. Again from comparison of the relative thickness change to predicted change from FTIR (loss in 2960 cm^{-1} band), we conclude we did not have enough results on the early stages (much earlier

than 50 h) to distinguish the crossover from the early to intermediate stages. The correlation between film thickness and the mass changes measured by FTIR no longer followed a linear relationship, i.e. we have only observed the intermediate and final degradation stages.

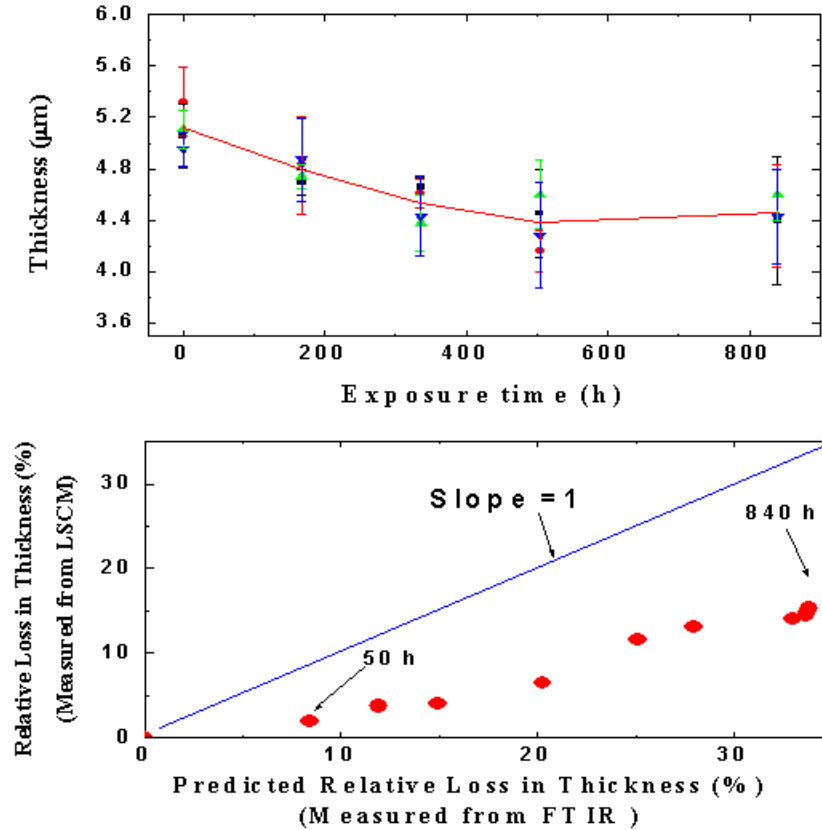


Figure 12. Upper graph: the measured film thickness of six AM coatings as a function of exposure time. The line is the averaged values of six samples; bottom graph: comparison between the predicted relative loss in thickness from FTIR peak at 2960 cm^{-1} and the relative loss in film thickness measured by LSCM. The estimated uncertainty of data in the bottom graph is about 10 % mostly due to the uncertainty in the film thickness measurement, especially in the late stages.

Figure 13a shows the surface morphology of three different AM samples after the same exposure time. Although these three samples were cut from the same larger spin-casted specimen, the rate of local degradation/surface deformation is different. The difference in surface morphology at the intermediate/late stages for different samples is noticeable, but it is less noticeable in the thickness and FTIR absorbance measurements. That is, the progress of degradation can be monitored more closely by the surface morphology measurement. In other words, monitoring the local surface deformation can provide insights into the mode of degradation. Figure 13b shows the time evaluation of the surface deformation at four different exposure times, starting smooth and featureless at zero exposure time. In addition to some small pits observed similar to the exposed AU coatings, there were islands and some underlying network-type of microstructures in the

immediate stage of the degradation process. These microstructures evolved and surface roughness of the coating increased as observed in the AFM measurements (Figure 14).

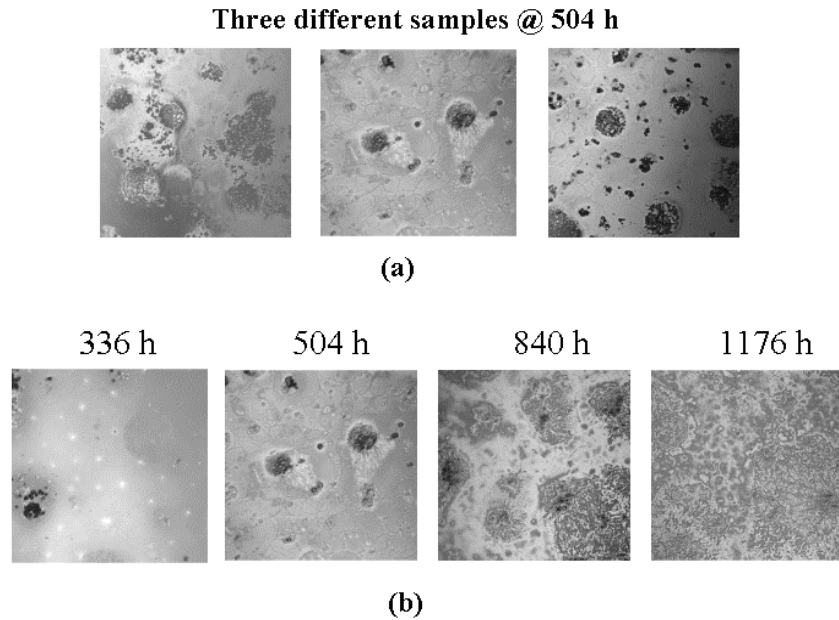


Figure 13. (a) LSCM images of three different AM coatings at the same exposure time (504 hours). (b) Time evolution of surface deformation of an AM coating at four different exposure times. Each LSCM micrograph is 184 μm by 184 μm by size.

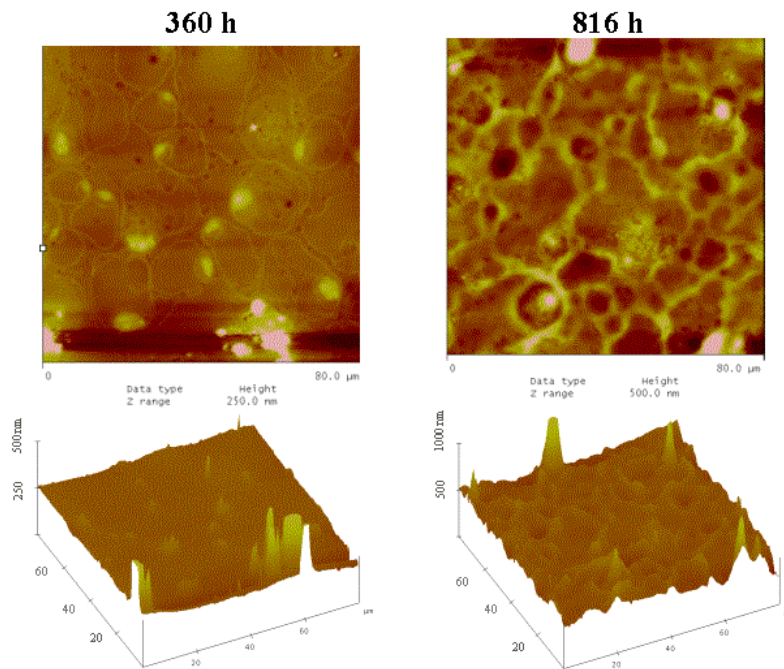


Figure 14. AFM images of AM coatings at two different exposure times.

Concluding Remarks

We have demonstrated the use of laser scanning confocal microscopy as a non-destructive characterization tool for measuring surface morphology and film thickness changes in two coating systems during exposure to UV environments. The relationship between the chemical and physical changes has been investigated. It was found that the mass changes (CH 2960 cm^{-1} band) measured by FTIR only correlated to the film thickness changes measured by LSCM in the early stage of the degradation process. The time frame for pit formation and the onset of the early to intermediate stages of the degradation for the AU system is less than 400 h, but less than 50 h for the AM system. More measurements in characterization of pit size and other microstructure as a function of exposure time will be conducted using a combination of AFM and LSCM techniques. On going research also includes: 1) exploring the interfacial heterogeneous hypothesis to investigate the origin and formation of pits and their degradation mechanism, 2) relating the surface roughness to the gloss measurements, 3) calculating the optical reflectance from measured surface morphology using Ray scattering model. With the continuous efforts in measurements and theoretical modeling, we might be able to establish a “direct” method to investigate the relationship between physical and chemical degradation of coatings exposed to weathering conditions.

Reference

1. D.R. Bauer and J.W. Martin, eds., Service Life Predication of Organic Coatings: A Systems Approach, ACS Symposium Series **722**, (Oxford University Press, 1999).
2. K. M. Wernstahl, “Service Life Prediction of Automotive Coatings, Correlating Infrared Measurements and Gloss Retention,” *Polym. Degrad. Stab.* **54**, 57 (1996).
3. J. L. Gerlock, C. A. Smith, V. A. Cooper, T. G. Dubiber, W. H. Weber, “On the Use of Fourier Transform Infrared Spectroscopy and Ultraviolet Spectroscopy to Assess the Weathering Performance of Isolated Clearcoats from Different Chemical Families,” *Polym. Degrad. Stab.* **62**, 255 (1998).
4. J. Martin, T. Nguyen, E. Byrd, B. Dickens, and N. Embree, “Relating Laboratory And Outdoor Exposures of Coatings: I. Cumulative Damage Model and Laboratory Experiment Apparatus,” *Polym. Degrad. Stab.*, **75**, 193 (2002).
5. T. Nguyen, J. Martin, E. Byrd, and N. Embree, “Relating Laboratory And Outdoor Exposures of Coatings: II. Effects of Relative Humidity on Photodegradation of Acrylic Melamine,” *J. Coatings Technology*, **74**, No. 932, 31 (2002).
6. S. G. Croll and A.D. Skaja, “Quantitative Spectroscopy to Determine the Effects of Photodegradation on a Model Polyester-Urethane Coatings” FSCT·ICE 2002 Proceedings of the 80th Annual Meeting Technical Program, Oct. 30 – Nov 1, New Orleans, LA. (2002).
7. C. A. Smith, J. L. Gerlock, A. V. Kucherov, T. Misovski, C. M. Seubert, R. O. Carter III, and M. E. Nichols, “Evaluation of Accelerated Weathering Tests for Automotive Clears Using Transmission Fourier Transform Infrared Spectroscopy,” FSCT·ICE

2002 Proceedings of the 80th Annual Meeting Technical Program, Oct. 30 – Nov 1, New Orleans, LA. (2002).

8. M. Osterhold and P. Glöckner, "Influence of Weathering on Physical properties of Clearcoats," *Prog. In Organ. Coatings*, **41**, 177 (2001).
9. M. A. Johnson and P. J. Cote, "Detrended Fluctuation Analysis of UV Degradation in a Polyurethane Coatings," *J. Coatings Technology*, **75**, No. 941, 51 (2003).
10. M.R. VanLandingham, T. Nguyen, W. E. Byrd, and J. W. Martin, "On the Use of the Atomic force Microscope To Monitor Physical Degradation of Polymeric Coating Surfaces," *J. Coatings Technology*, **73**, No. 923, 43 (2001).
11. M. E. McKnight, E. Marx, M. Nadal, T. V. Vorburger, P. Y. Barnes, M. A. Galler, "Measurements and Predictions of Light Scattering by Clear Epoxy Coatings," *Applied Optics*, **40**, No. 13, 2159 (2001).
12. L. Sung, M. E. Nadal, M. E. McKnight, E. Marx, and B. Laurenti, "Optical Reflectance Of Metallic Coatings: Effect Of Aluminum Flake Orientation," *J. Coatings Technology*, **74**, No. 932, 55, (2002).
13. F. Y. Hunt, E. Marx, G. W. Meyer, T. V. Vorburger, P. A. Walker, and H. B. Westlund "A First Step Towards Photorealistic Rendering of Coated Surfaces and Computer Based Standards of Appearance ", in Service Life Prediction: Methodology and Metrologies, J. W. Martin and D. R. Bauer, eds., ACS Symposium Series **805** (Oxford University Press, 2002).
14. T.R. Corle, G.S. Kino, Confocal Scanning Optical Microscopy and Related Imaging Systems (Academic Press 1996).